Semiconductors, 2023, Vol. 57, No. 6

Plasma enhanced atomic layer deposition of InP layers and multilayer InP/GaP structures on Si substrate

© A.S. Gudovskikh[1,2], A.V. Uvarov[1], A.I. Baranov[1], E.A. Vyacheslavova[1], A.A. Maksimova[1,2], D.A. Kirilenko[3]

[1] Alferov Federal State Budgetary Institution of Higher Education and Science Saint Petersburg National Research Academic University of the Russian Academy of Sciences,
194021 St. Petersburg, Russia
[2] St. Petersburg State Electrotechnical University „LETI"
197376 St. Petersburg, Russia
[3] Ioffe Institute,
194021 St. Petersburg, Russia
E-mail: gudovskikh@spbau.ru

Received August 24, 2023
Revised September 1, 2023
Accepted September 1, 2023

For the first time, InP layers were grown on Si substrates at a temperature of 380°C using the plasma-enhanced atomic layer deposition. According to X-ray diffraction analysis and transmission electron microscopy, the layers are microcrystalline with a grain size of 20−30 nm and a preferred orientation (111). Raman spectra exhibit clearly distinguish the LO peak at 341.9 cm^{-1}, which is characteristic of crystalline InP. Microcrystalline InP layers grown on fused silica substrates demonstrated a high photoconductivity of 2.3 $\Omega^{-1} \cdot cm^{-1}$ under solar spectrum AM1.5G (100 mW/cm^2) illumination. The study of the growth of layers of binary compounds InP and GaP in one process of plasma-enhanced atomic layer deposition demonstrated the fundamental possibility of controlling the composition of InP/GaP digital alloy. The InP/GaP digital alloys are characterized by the coalescence of the LO peaks of InP (341.9 cm^{-1}) and GaP (365 cm^{-1}) in the Raman spectra. Increase of GaP component in the layer leads to boarding of this feature in the Raman spectra due to a shift of the edge towards the GaP peak (402 cm^{-1}). A study of the optical properties by transmission and reflection measurements of microcrystalline InP/GaP digital alloy layers deposited on transparent substrates demonstrated the possibility of varying the optical gap in the range of 1.3−2 eV.

Keywords: GaP, InP, atomic layer deposition, heterostructures, photoconductivity.

DOI: 10.61011/SC.2023.06.57157.22k

1. Introduction

Integration of compounds $A^{III}B^{V}$ with Si makes it possible to create new optoelectronic devices, such as light-emitting diodes, optical integrated circuits and multi-junction solar cells. The most suitable material for growth on a Si substrate is GaP from a technological point of view. This is due to the fact that GaP has the smallest among all binary compounds $A^{III}B^{V}$ mismatch of the crystal lattice parameters with Si (0.36% at room temperature). Therefore, GaP is actively used as a nucleation layer for the growth of compounds $A^{III}B^{V}$ on Si substrates. At the same time, the GaP band gap width (2.26 eV) is significantly larger than silicon, which makes it possible to use GaP as a wide-band emitter for phototransformation structures based on Si [1–4]. It is also important that for GaP, the gap of the conduction bands with Si is only 0.25 eV, which eliminates the occurrence of undesirable barriers at the interface of the heterojunction n-GaP/p-Si [5–9]. However, GaP is a non-direct-band semiconductor, which greatly limits its use as active layers of optoelectronic devices. In this regard, multilayer structures grown on a silicon substrate consisting of a combination of layers of non-direct gap and straight-band compounds, for example quantum wells InP [10], are of interest. The use of a sequence of layers in the form of short-period InP/GaP superlattices (digital solutions) can potentially provide accurate control of the effective band gap width required to achieve optimal transition matching.

However, if we consider the use of solar radiation in photovoltaic converters, then the technology of forming such devices should provide the possibility of large-scale production with minimal energy consumption. Promising results for solar energy have been achieved on the growth of microcrystalline InP layers, which have sufficiently high values of the lifetime of charge carriers [11,12]. However, the technological approaches used to form layers require relatively high temperatures (> 500°C) and do not allow varying the composition of layers to control the band gap.

A low-temperature technological approach consisting in the use of plasma chemical atomic layer deposition is considered in this paper as a method of synthesis of layers $A^{III}B^{V}$. This technique provides the potential for precision control of the composition of layers in conditions of large-scale production. Previously, microcrystalline layers of GaP [13,14] were grown using this method, and providing initial (first 20 nm) epitaxial growth on silicon [15].

2. Experimental

GaP, InP layers and multilayer InP/GaP structures were formed by atomic layer plasma chemical deposition on

crystalline silicon substrates with $(100)n$- and p-orientations of the conductivity type, as well as on quartz substrates. The method of plasma chemical atomic layer deposition was implemented using Oxford Plsmalab 100 PECVD system. Trimethylindium (TMI) and trimethyl gallium (TMG), respectively, were used as a source of In and Ga, and — phosphine (PH_3) was used as a source of phosphorus. Decomposition of TMI and TMG occurred due to temperature, and decomposition of phosphine (PH_3) in plasma of HF (13.56 MHz) discharge with a power density of 90 μW/cm^2. The layers were grown at a pressure of 350 mTorr and a temperature of 380°C. The substrate temperature was chosen so that it meets two conditions: 1) sufficiency for evaporation of phosphorus atoms not bound to gallium or indium, i.e. a monolayer (ML) of phosphorus was formed on the surface; 2) ensuring thermal decomposition of organometallic compounds (TMI, TMG) on the surface of the growing film. The doses of organometallic compounds and phosphine in one cycle were 50 and 0.5 nmol $\cdot$ cm^2, respectively. Earlier studies of the dependence of the growth rate on the dose of precursors in one cycle for GaP have shown that these conditions provide a regime of atomic layer deposition of [15]. The thickness of the GaP layer formed in one cycle is equal to 0.1 ± 0.01 nm (~ 0.5 monolayer), while the growth rate of InP layers is much higher and is 0.17 ± 0.01 nm (~ 0.7 monolayer) for one cycle.

Two InP/GaP structures were grown with the same values of the total thickness of ~ 35 nm. The first structure is a digital solid solution, where one GaP deposition cycle alternated with one InP deposition cycle. The structure can be represented as a periodic combination of 0.5 GaP monolayer and 0.7 InP monolayer (0.5 GaP ML/0.7 InP ML) taking into account the growth rates. The second structure is a periodic combination of 15 GaP monolayers and 4.2 monolayer InP (15 GaP ML/4.2 InP ML).

The thicknesses and morphology of the layers were studied using scanning electron microscopy (SEM) using a Supra 25 Zeiss microscope. The structural properties were studied using X-ray diffractometry, transmission electron microscopy (TEM) (Jeol JEM-2100F microscope), as well as Raman spectroscopy using a laser at a wavelength of 532 nm (EnSpectr R532 spectrometer). Optical properties were studied using the results of measuring the transmission and reflection spectra of layers deposited on quartz substrates in the wavelength range 400–1200 nm. Silver contacts were applied to the surface of the InP layer deposited on quartz substrates by thermal vacuum spraying through a free mask to study the photovoltaic properties.

3. Results and discussion

The image of the chip of the InP layer deposited on the Si substrate obtained at an angle 20° using the scanning electron microscopy method is shown in Figure 1. The InP layer has a granular structure with a rough surface characteristic of microcrystalline GaP layers [13,14].

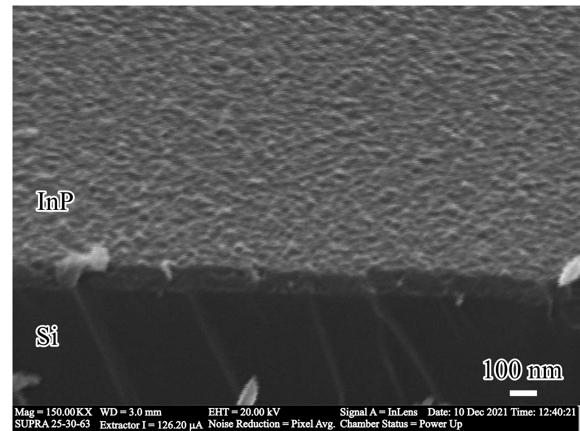

Figure 1. SEM image of the chip of the InP layer deposited on the Si substrate, obtained at an angle of 20°.

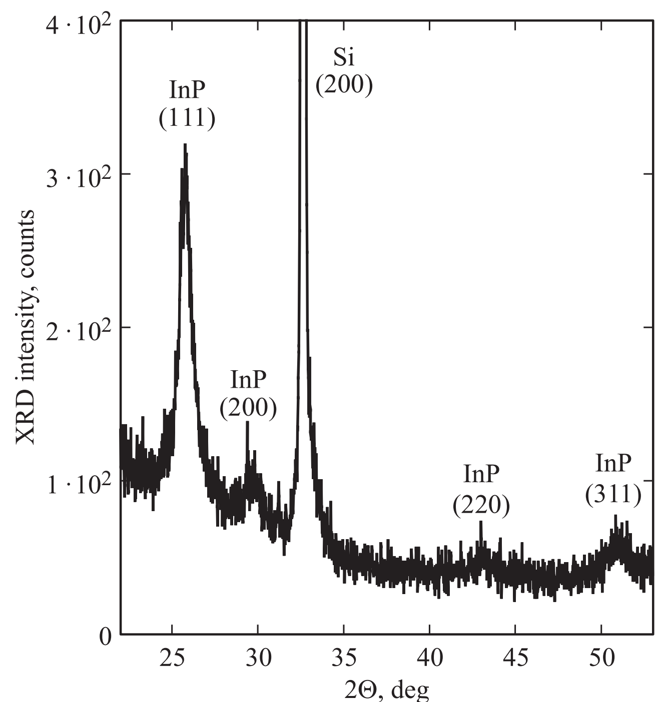

Figure 2. Diffractogram of the InP layer deposited on the Si substrate.

The study of the structural properties of InP using X-ray diffraction analysis confirms their microcrystalline structure. There are reflexes corresponding to the InP with the crystal structure of the zinc blende on the diffractogram shown in Figure 2, in addition to the response from the silicon substrate [11]. It is possible to differentiate responses from various crystallographic planes (111), (100), (110) and (311) on the diffractogram, which indicates the microcrystalline structure of the InP layer grown on the Si substrate. However, the dominance of the peak of (111) suggests that InP nanocrystallites have a predominant orientation in the direction of (111).

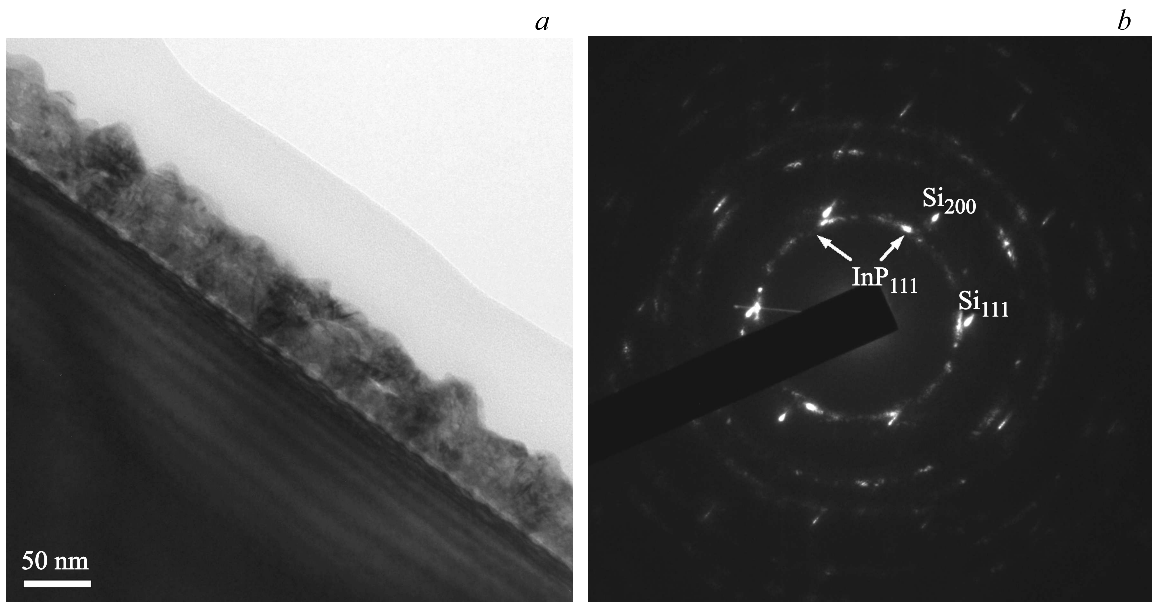

Figure 3. An image of the InP layer on a Si substrate obtained by transmission electron microscopy (*a*), and an image of electron diffraction (*b*).

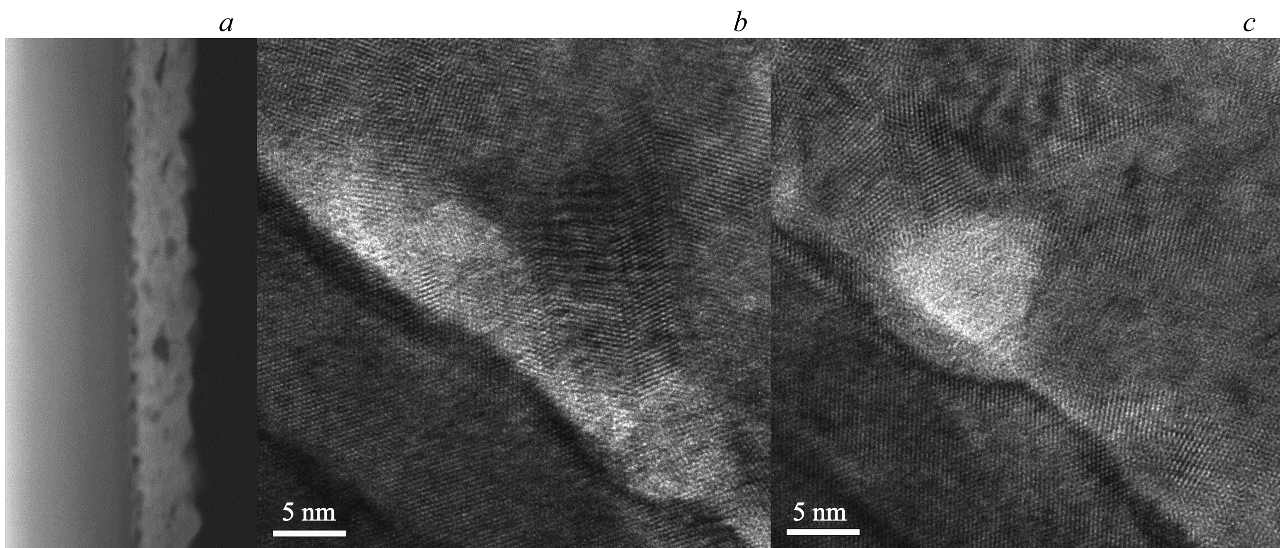

Figure 4. HAADF–STEM images of InP layer on Si (*a*) and high-resolution TEM (*b, c*) interface Si/InP.

Studies conducted using transmission microscopy (Figure 3) confirm the results of X-ray diffraction analysis. The InP layer consists of disoriented nanocrystallites of the size 20–30 nm, having a predominant orientation in the direction of (111) according to the image of the cross-section of the InP layer on the Si substrate (Figure 3, *a*) and the selected area electron diffraction (SAED) (Figure 3, *b*). The fundamental difference for microcrystalline InP and GaP layers grown by atomic layer plasma chemical deposition on Si substrate is the absence of two-dimensional epitaxial growth of InP at the initial stage, characteristic of GaP [15]. Obviously, this is primarily due to the significant difference in the parameters of the crystal lattices between InP and Si. In addition, as shown by studies using a scanning TEM in a dark field with a large angle (HAADF–STEM) of the InP layer on Si and High-resolution TEM (Figure 4), voids are observed at the InP/Si interface, and pits are present on the substrate surface in the places of voids. The formation of pits on the surface of Si apparently occurs as a result of etching of Si during the growth of the InP layer. It should be noted that the etching effect is not observed when GaP grows on Si under similar conditions when GaP grows on Si under similar conditions [15]. Additional studies are planned to determine the causes of the observed effect.

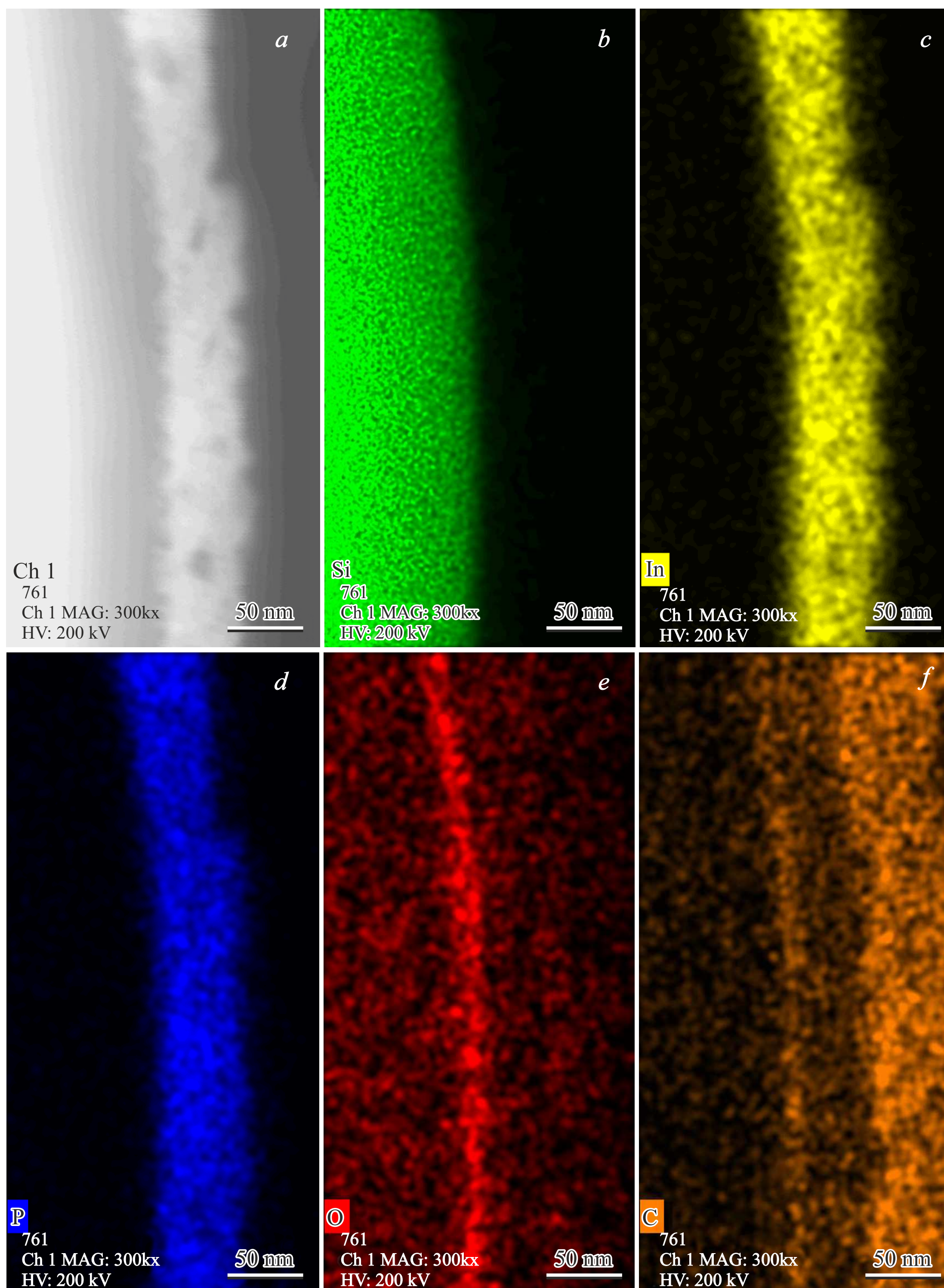

Figure 5. TEM image of the InP layer on the Si substrate (*a*) and the distribution maps of the main elements for this area: Si (*b*), In (*c*), P (*d*), O (*e*), C (*f*). (A color version of the figure is provided in the online version of the paper).

Figure 5 shows the distribution maps of the main elements for the InP layer on Si obtained by energy dispersive X-ray spectroscopy are presented. It should be noted that phosphorus and indium are distributed fairly uniformly over the InP layer. There is no excessive concentration of these elements at the interface with the substrate within the limits of the resolution of the technique. Quantitative estimates of the spectra of energy dispersive X-ray spectroscopy indicate that the composition of the InP layers is close to stoichiometric within the measurement error. There is an

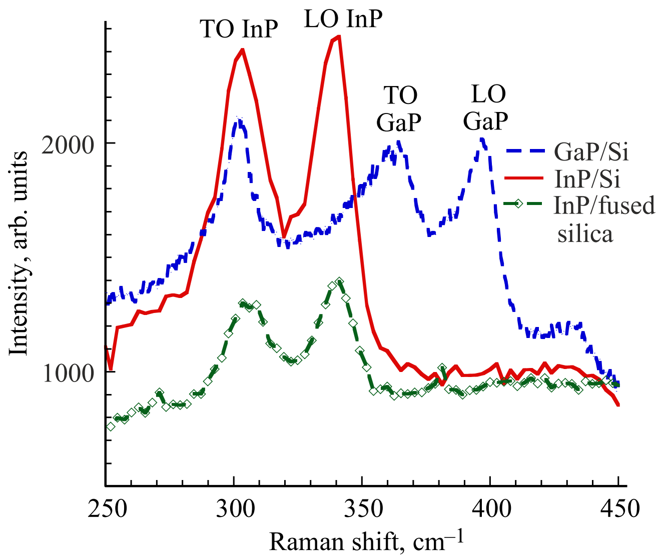

Figure 6. The Raman scattering spectra of InP layers on Si and quartz substrates. The GaP spectrum grown on Si is given for comparison.

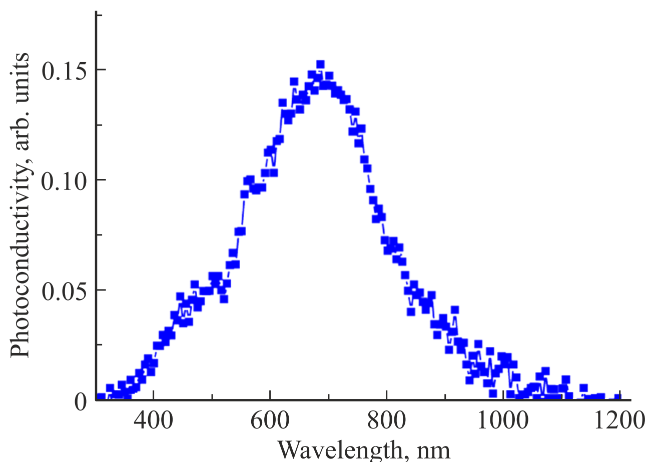

Figure 7. The photoconductivity spectrum of the InP layer on a quartz substrate.

increased concentration of oxygen and carbon at the InP/Si interface, which may be associated with the formation of voids. The presence of oxygen, carbon, and silicon is not observed in the InP layer itself within the sensitivity of the technique. It should be noted that for oxygen (O) and carbon (C) the signal is received at the limit of the detecting ability and on the distribution maps (Figure 5, *e,f*) the background signal is visible both in the InP layer and in the Si substrate. The equally low level of the signal detected in the InP layer and the Si substrate indicates that the concentration of these elements is below the level of determining ability.

RS spectroscopy is of great importance for the analysis of structural properties, since this method allows for non-destructive rapid diagnostics of thin polycrystalline layers deposited on various substrates. Figure 6 shows the RS spectra for InP layers deposited on Si and quartz substrate, and the spectrum of the microcrystalline GaP layer on the substrate is also given for comparison [13]. The peak LO at 347 cm^{-1}, characteristic of the crystalline InP [16], is clearly distinguishable on the RS spectra of the microcrystalline InP layer on Si. Another peak TO characteristic of InP at 303.7 cm^{-1} merges with the response from the Si substrate at 307 cm^{-1}, which significantly complicates its identification. The spectrum of the InP layer grown on a quartz substrate also has two peaks characteristic of crystalline InP (TO and LO), which indicates that this layer is also microcrystalline. The microcrystalline GaP is characterized by the presence of two peaks at 365 and 402 cm^{-1}, corresponding to the doublet TO–LO of the crystalline GaP [17].

The photovoltaic properties of microcrystalline InP were studied with respect to layers deposited on a nonconducting quartz substrate to avoid any impact of the substrate. Measurements of the photoconductivity of the InP layer with a thickness of 70 nm when illuminated by the solar spectrum AM1.5 G (100 μW/cm^2) gave the value 2.3 $\Omega^{-1}\cdot\mathrm{cm}^{-1}$. The obtained value exceeds the photoconductivity of amorphous and microcrystalline silicon by several orders of magnitude at the same generation level ($\sim 10^{22}\,\mathrm{cm}^{-3}\cdot\mathrm{c}^{-1}$) [18,19], which indicates higher values of the product of mobility and lifetime ($\mu\tau$) for microcrystalline layers InP. High values of the product $\mu\tau$ are one of the key requirements for the layers used in thin-film photovoltaic solar radiation converters [20]. The spectral dependence of the photoconductivity is shown in Figure 7. The photosensitivity spectrum of the layer corresponds to what is expected for InP and is in the range of 350–950 nm, which is of interest for the creation of photovoltaic converters. However, if we consider the application for multi-junction solar cells with a lower junction formed on the basis of silicon, then the absorption edge of the upper junction should be shifted to the short-wave region.

The absorption edge can be shifted by the formation of GaInP solid solutions or short-period InP/GaP superlattices. Both approaches were implemented by integrating the growth of layers of binary compounds InP and GaP in one process of atomic-layer plasma chemical deposition. Figure 8 shows images obtained using SEM for layers of digital solid solution (0.3 GaP ML/0.7 InP ML) and short-period superlattice InP/GaP (15 GaP ML/4.2 InP ML), grown on a Si substrate. Microcrystalline layers have a granular structure with a grain size of 30–50 nm. The results of measurements of energy dispersive X-ray spectroscopy indicate an increasing concentration of Ga with an increase in the ratio of the number of monolayers InP/GaP, however, numerical estimation of the concentration is difficult due to the too small thickness of the layers.

Digital solid solutions of InP/GaP are characterized by the merging of LO peaks of InP (347 cm^{-1}) and GaP (365 cm^{-1}) on the RS spectra shown in Figure 9. At

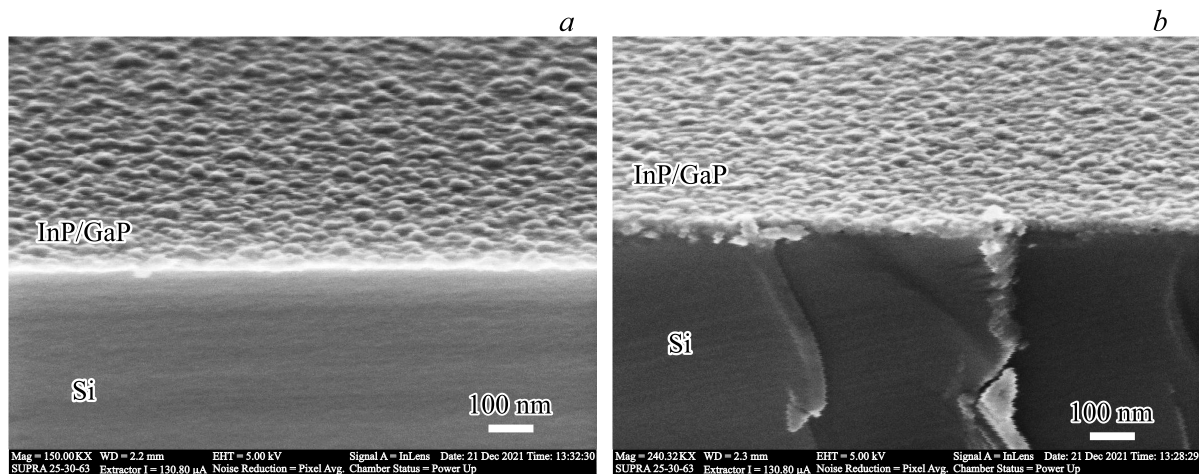

Figure 8. SEM images of a digital solid solution (0.3 GaP ML/0.7 InP ML) and a GaP/InP short-period superlattice (15 GaP ML/4.2 InP ML) grown on a Si substrate.

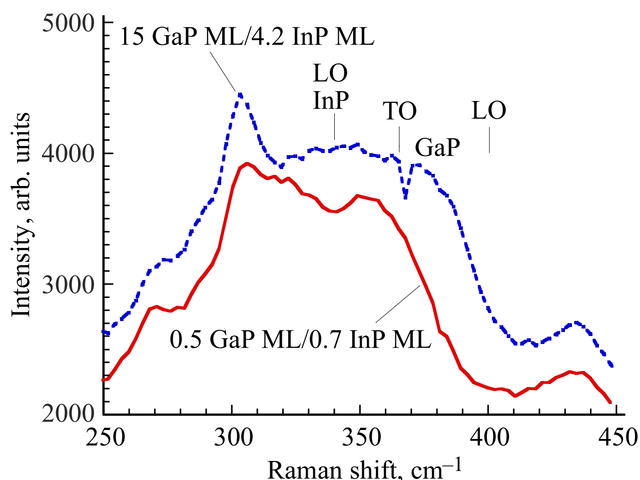

Figure 9. The Raman scattering spectrum of a digital solid solution (0.3 GaP ML/0.7 InP ML) and a GaP/InP short-period superlattice (15 GaP ML/4.2 InP ML) grown on a Si substrate.

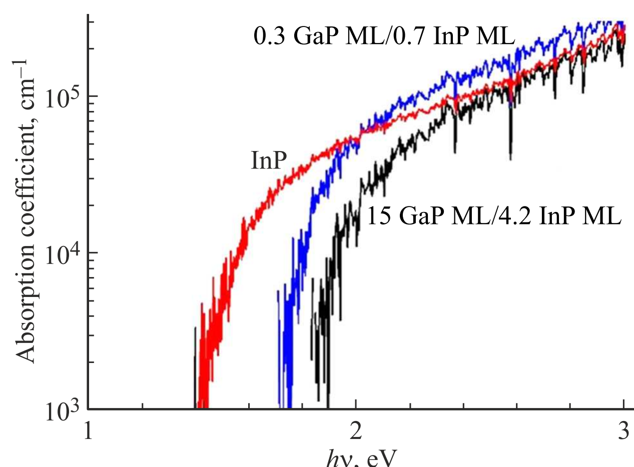

Figure 10. Spectral dependence of the absorption coefficient for InP layers and InP/GaP solid solutions.

the same time, the expansion of the response from the layer due to shift of the edge towards TO peak GaP ($402\,cm^{-1}$) is observed with an increase of the GaP concentration.

Optical properties of InP layers and multilayer InP/GaP structures deposited on transparent substrates were studied. Spectral dependences of the transmittance coefficient were obtained based on the measurement results of the transmission and reflection spectra as shown in Figure 10. It can be seen that the absorption edge shifts towards high energies with an increase of the GaP fraction. Thus, the principal possibility of variation of the optical band gap width in a sufficiently wide range of 1.3−2 eV is demonstrated due to variation in the ratio of the number of monolayers of binary compounds InP and GaP in one process of atomic-layer plasma chemical deposition.

4. Conclusion

For the first time, InP layers and digital solid solutions of InP/GaP were grown using the method of atomic layer plasma chemical deposition on Si substrates. Studies using X-ray diffraction analysis and electron microscopy have shown that the films have a microcrystalline structure with a predominant orientation of (111). Microcrystalline InP layers have demonstrated a high value of photoconductivity, which determines the prospects of this material for use in photovoltaic converters operating in the wavelength range 350−950 nm. The absorption edge can be shifted to the short-wave side through the use of digital solid solutions InP/GaP. The possibility of variation of the optical band gap width in the range 1.3−2 eV was demonstrated by the studies by measuring the transmission and reflection of optical properties of layers of digital solid solutions InP/GaP deposited on transparent substrates.

Funding

This study was carried out under state assignment of the Ministry of Science and Higher Education of the Russian Federation (project No. FSRM-0791-2023-0007).

Conflict of interest

The authors declare that they have no conflict of interest.

References

[1] P. Caño, C.M. Ruiz, A.L. Navarro, B. Galiana, I. García, I. Rey-Stolle. Solar Cells. Coatings, **11** (4), 398 (2021).
[2] D.L. Lepkowski, T.J. Grassman, J.T. Boyer, D.J. Chmielewski, Ch. Yi, M.K. Juhl, A.H. Soeriyadi, N. Western, H. Mehrvarz, U. Römer, A. Ho-Baillie, Ch. Kerestes, D. Derkacs, S.G. Whipple, A.P. Stavrides, S.P. Bremner, S.A. Ringel. Sol. Energy Mater. Solar Cells, **230**, 111299 (2021).
[3] J.T. Boyer, A.N. Blumer, Z.H. Blumer, D.L. Lepkowski, T.J. Grassman. J. Cryst. Growth, **571**, 126251 (2021).
[4] A. Navarro, E. García-Tabarés, Q.M. Ramasse, P. Caño, I. Rey-Stolle, B. Galiana. Appl. Surf. Sci., **610**, 155578 (2023).
[5] I. Sakata, H. Kawanami. Appl. Phys. Express, **1**, 091201 (2008).
[6] P. Perfetti, F. Patella, F. Sette, C. Quaresima, C. Capasso, A. Savoia, G. Margaritondo. Phys. Rev. B, **30**, 4533 (1984).
[7] A.D. Katnani, G. Margaritondo. Phys. Rev. B, **28**, 1944 (1983).
[8] O. Romanyuk, T. Hannappel, F. Grosse. Phys. Rev. B, **88**, 115312 (2013).
[9] A.S. Gudovskikh, A.I. Baranov, A.V. Uvarov, D.A. Kudryashov, J.-P. Kleider. J. Phys. D: Appl. Phys., **55**, 135103 (2022).
[10] F. Hatami, W.T. Masselink, J.S. Harris. Nanotechnology, **17**, 3703 (2006).
[11] R. Kapadia, Z. Yu, H.H. Wang, M. Zheng, C. Battaglia, M. Hettick, D. Kiriya, K. Takei, P. Lobaccaro, J.W. Beeman, J.W. Ager, R. Maboudian, D.C. Chrzan, A. Javey. Sci. Rep., **3**, 2275 (2013).
[12] W. Metaferia, Y.-T. Sun, S.M. Pietralunga, M. Zani, A. Tagliaferri, S. Lourdudoss. J. Appl. Phys., **116**, 033519 (2014).
[13] A.S. Gudovskikh, I.A. Morozov, A.V. Uvarov, D.A. Kudryashov, E.V. Nikitina, A.S. Bukatin, V.N. Nevedomskiy, J.-P. Kleider. J. Vac. Sci. Technol. A, **36**, 21302 (2018)
[14] S. Yun, C.-H. Kuo, P.-C. Lee, S.T. Ueda, V. Wang, H. Kashyap, A.J. Mcleod, Z. Zhang, C.H. Winter, A.C. Kummel. Appl. Surf. Sci., **619**, 156727 (2023).
[15] A.V. Uvarov, A.S. Gudovskikh, V.N. Nevedomskiy, A.I. Baranov, D.A. Kudryashov, I.A. Morozov, J.-P. Kleider. J. Phys. D: Appl. Phys., **53**, 345105 (2020).
[16] M.J. Seong, Olga I. Mićić, A.J. Nozik, A. Mascarenhas, Hyeonsik M. Cheong. Appl. Phys. Lett., **82**, 185 (2003).
[17] S. Hayashi. Sol. St. Commun., **56**, 375 (1985).
[18] A. Madan, M.P. Shaw. *The Physics and Applications of Amorphous Semiconductors* (Boston–San Diego–N.Y.–London–Sydney–Tokyo–Toronto, Academic Press, 1988).
[19] M. Goerlitzer, N. Beck, P. Torres, J. Meier, N. Wyrsch, A. Shah. J. Appl. Phys., **80** (9), 5111 (1996).
[20] N. Beck, N. Wyrsch, Ch. Hof, A. Shah. J. Appl. Phys., **79** (12), 9361 (1996).

Translated by A.Akhtyamov